Life-Cycle Cost Assessment of Conventional and Hybrid Sliding-Rocking Bridges in Seismic Areas

Jakub Valigura[1], Abbie B. Liel[2] and Petros Sideris[3]
[1]Structural Engineer, KPFF Consulting Engineers, San Francisco, CA
(formerly Ph.D. Candidate, Univ. of Colorado Boulder)
jakub.valigura@kpff.com
[2]Associate Professor, University of Colorado, Boulder, CO 80304
abbie.liel@colorado.edu (corresponding author)
[3]Assistant Professor, Texas A& M University, College Station, TX 77845
petros.sideris@tamu.edu

Abstract

This paper investigates the impacts of the column system on bridge life-cycle costs in high seismic areas. It focuses on hybrid sliding-rocking (HSR) columns, which are an accelerated bridge construction (ABC) technology. The authors conduct a life-cycle cost assessment, quantifying costs of bridge construction and potential earthquake damage and subsequent repairs, as well as the cost of bridge closure time due to construction or repairs. Two prototypical modern seismically-designed bridges are considered, each designed with both conventional RC and HSR columns. Construction costs of HSR columns are higher. However, drift demands on the HSR columns are generally lower, damage is less severe and costs of repairing the columns are greatly reduced. Moreover, construction times are about 80% quicker for HSR columns, and repair times are reduced relative to conventional construction. The results suggest advantages in most cases to the HSR column system, reducing construction time and expected costs and time for seismic repairs sufficiently to counteract the increase in upfront construction costs. The benefits of the HSR, and by extension other ABC column systems, are particularly significant for highly trafficked bridges in high seismic areas, but hold for a wide range of input assumptions.

Keywords: Bridge construction, Earthquake engineering, Life-cycle costs, Concrete structures, Bridge design

1. Introduction

Many U.S. bridges are structurally deficient (9%), functionally obsolete (13%), or reaching the end of their useful life (ASCE, 2017) and significant bridge replacement, rehabilitation or retrofit will be needed in the coming years. Accelerated bridge construction (ABC) methods have the potential to support the needed improvement of bridge infrastructure. ABC uses innovative planning, design, materials, and construction methods, to reduce on-site construction time and, thus, delays to the traveling public associated with bridge construction/retrofits (Culmo 2011). The use of precast reinforced concrete (RC) segments (or preassembled steel segments) is critical for ABC because these segments can be quickly assembled to limit on-site disruption associated with construction.

Although ABC has been increasingly adopted for superstructures (*e.g.,* Caltrans 2008a; WSDOT 2018), for substructures, these application has been mostly limited to low seismic areas. This is primarily because of uncertainties about the performance of ABC substructure systems under strong earthquakes. However, the Washington Department of Transportation (WSDOT) recently built three bridges incorporating precast columns (WSDOT 2018), and Caltrans constructed a pilot multi-span precast bridge in 2017 with precast columns (Caltrans 2018). Both WSDOT and Caltrans reported lower on-site construction time compared to conventional construction. However, uncertainty remains about the seismic behavior of precast column systems (Culmo 2011), and potential benefits of ABC in seismic zones, including economic benefits, and safety, considering the entire service life of a bridge have not been quantified (WSDOT 2009).

There have been two major types of connections in ABC substructure systems proposed for applications high seismic areas. The first type uses prefabricated monolithic columns connected with the foundation and the cap beam through emulative (or monolithic) connections, such as bar coupler connections (e.g. Tazarv and Saiidi 2013), grouted duct connections (e.g. Restrepo et al. 2011), gap pocket connections (e.g. (Matsumoto et al. 2008)) and member socket connections (e.g. Lehman & Roeder 2012). The second type has dry rocking connections with internal unbonded post-tensioning (e.g. Hewes 2007), while energy dissipation mechanisms were introduced in the form of internal or external yielding rebar (e.g. Ou et al. 2010). The second type has been shown though experimental and numerical studies to result in much lower residual deformations and sustain less damage compared to conventional designs. The hybrid sliding-rocking (HSR) columns, which are our focus here, are of the first type. These columns have been shown to limit seismic demands and damage through the use of sliding joints over the column height, and provide low permanent residual drifts via their internal unbonded PT and end rocking joints (Salehi 2019; Sideris 2012; Sideris et al. 2014a, 2014b, 2015; Valigura 2019).

This study performs a comparative life-cycle cost assessment (LCCA) of RC bridges with conventional columns and HSR columns, in the presence of seismic hazard, in order to quantify the relative benefits of each structural system. This LCCA considers the initial costs of construction of the bridge, as well as the costs of repairing earthquake damage over the bridge's service life. This study assumes the bridges have a service life of 75 years, and considers both the direct costs of bridge construction and repairs, as well as the costs of bridge closure time during the initial construction and repairs of seismic damage. Although the analysis is specific to the HSR systems, implications for other seismically-designed ABC column systems are discussed.

2. Background

2.1 Seismic Behavior of the HSR Column System

Among the different types of ABC columns that have been proposed for seismic regions, the authors focus on HSR columns, introduced by Sideris (2012) and Sideris et al. (2014a, 2014b, 2015). Several precast RC segments, connected by internal unbonded PT strands to the foundation and cap beam, form the HSR column. The segments are allowed to rock at their column-to-foundation and column-to-cap beam joints. Intermediate sliding joints are distributed along the height of the column. For shaking intensities lower than about the design earthquake level, sliding is designed to dominate the response, while rocking is designed to remain negligible. At higher intensities, the rocking joints are activated and aim to prevent tension damage in the concrete and provide self-centering. Residual joint sliding present after the earthquake can be restored using hydraulic or mechanical means (Valigura 2019).

Sideris (2012) and Sideris et al. (2014a, 2014b, 2015) performed large-scale tests on the first version of HSR columns, which are herein termed "*Generation 1*". These tests included quasi-static lateral cyclic loading on individual cantilever HSR columns, and shake table testing of a bridge with HSR columns. The experiments demonstrated the superior seismic performance of the HSR columns compared to conventional RC columns. In particular, these tests reported lower peak and residual drift demands, and lower extent of damage than expected for conventional columns. The sliding joints provide significant energy dissipation, which limits the displacement demands to the system (Sideris et al. 2014a, 2015).

The design of HSR columns has been refined to further limit damage in the "*Generation 2"* HSR columns. These *Generation 2* columns, illustrated in Figure 1, have a lower number of sliding joints unevenly distributed along the height. Also, the system is designed such that joint sliding initiates prior (or close) to the onset of rocking at the bottom. Furthermore, the sliding interface is a PTFE("*Teflon*")-on-PTFE surface, lowering the coefficient of friction to about 0.05. These design enhancements lower the damage to the columns, and reduce displacement demands even further due to higher effective damping, providing damping of 10-50% depending on the level of shaking (Salehi 2019). Salehi (2019) and Valigura (2019) tested large-scale "*Generation 2"* HSR columns under quasi-static cyclic lateral loading, showing that they performed as designed*, i.e.* exhibiting minimal damage at 2% drift ratio demands that represented a 2500-year hazard level, and experienced less damage than conventional columns for the same level of drift. Valigura (2019) further demonstrated that the columns could be adequately repaired if damage does occur. These studies also implied that the safety of the columns is satisfactory, with severe damage or collapse happening at drift ratios exceeding 8%.

Valigura (2019) also surveyed bridge engineering experts about HSR columns. The expert panel included eight participants, including four academics and four practicing bridge engineers with experience with bridge design in high-seismic areas. (For more information on the expert panel participant background and experience, refer to Valigura (2019). The experts expected on-site construction time of HSR columns to be 25% to 75% percent of construction time of conventional columns, but construction costs to be increased by about 50%. However, those surveyed suggested that the construction costs of HSR columns would likely eventually decrease as the process becomes more standardized. The experts expected that repair costs and times in a given earthquake would be lower for HSR columns, because of the HSR's damage avoidance characteristics. The panelists did suggest that the HSR system may require more regular maintenance (and perhaps shorter inspection intervals) than conventional columns, though they suggested that this extra maintenance could be avoided if sliding joints were sealed.

2.2 Previous Performance Assessments of ABC Bridge Column Systems

Research on ABC bridge column systems for high seismic areas has shown that there are benefits to many of these systems compared to conventional CIP column construction, because of their lower residual drift demands, *e.g.,* Sakai and Mahin (2004), lower damage, *e.g.,* Tazarv and Saiidi (2014), or both, *e.g.,* Sideris (2012). As an example of the beneficial behavior, Sakai and

Mahin (2004) reported, based on simulations, that PT columns limited the residual drifts to 14% of what an equivalent CIP column would experience, though they observed that the peak drifts were higher than for conventional columns. This observation is in agreement with general conclusion that rocking systems have larger peak displacement demands unless additional energy dissipating mechanisms are present, *e.g.*, Motaref et al. (2011), Ou et al. (2010). However, systems with additional energy dissipating mechanisms, like the HSR columns, can have lower peak displacement demands.

However, LCCA that consider construction and repair costs over the entire lifetime of the structure, are needed to provide a meaningful comparison between systems (WSDOT, 2009). The framework of performance-based earthquake engineering (PBEE), combined with LCCA, can be used to make these assessments. PBEE, *e.g.,* Deierlein et al. (2003), combines seismic hazard assessment with simulation of seismic demands on structures to quantify performance through metrics relevant to decision makers. For bridges, this framework has been used to evaluate the costs of earthquake-related repairs (*e.g.,* Mackie and Stojadinovic, 2005; Mackie et al., 2008; Yang et al., 2009), compare effectiveness of seismic retrofit strategies (*e.g.,* Padgett and DesRoches, 2009; Billah et al., 2013, Tapia and Padgett, 2016), and assess alternative repair strategies (*e.g.,* Valigura et al. 2019b). Of particular interest here are applications of PBEE to compare competing design strategies for new bridges. For example, Lee and Billington (2011) quantified the repair costs and time for CIP columns and unbonded PT bridge columns suggesting that, for a given level of shaking, the repair costs of the PT system were slightly higher, but the repair times were significantly lower.

Another assessment of an ABC column system is provided by Mashal and Palermo (2019), who examined the performance of the Wigram-Magdala Link Bridge in New Zealand based on empirical data and field observations. This bridge's columns have preassembled steel shells filled with concrete, with dissipative controlled-rocking connections at their connection to the foundation and superstructure. The bridge was estimated to cost about 2.5% more than conventional construction, but was completed six weeks ahead of schedule. During the 2016 Kaikoura earthquake, the bridge experienced no apparent damage, despite moderate to significant damage to other bridges in the region.

Additional (potential) advantages of ABC systems that can be evaluated through LCCA are the time saved during construction and while repairing any seismic damage. Bridge closure for construction and repairs can have significant economic effects in the form of detours, delays and trips not taken (Moore et al., 2006). For example, Abudayyeh et al. (2010) compared the construction time of a bridge that used ABC precast construction for columns, superstructure, pier caps, and abutments, to that of a similar conventional CIP bridge. They estimated that the ABC system would take 42% or 45 fewer days than the CIP bridge to construct. For the location/bridge of interest, they calculated that this time translated into $972,000 of savings.

3. Life-Cycle Assessment Methods

3.1 Goals and System Boundary

LCCA is an economic analysis of a structure that includes not only the initial construction costs, but also costs due to operation, inspection, maintenance, repair, and failure over its lifetime (Frangopol and Liu, 2007). This study applies LCCA to compare two structural systems, referred to here as *baseline* and *competing* systems. Our baseline system is a conventional bridge with CIP columns and superstructure. The competing system replaces the CIP columns with the ABC HSR columns. All other properties of the bridge are kept constant such that any change in the LCCA outcome between the systems can be attributed to the change in column design.

LCCA considers the major stages of a bridge's lifespan, outlined in Figure 2. It accounts for the economic impact of the upfront construction of the bridge, as well as seismic repairs, including both the cost expended in carrying out the construction or repair, and the time taken to conduct the repair. The study excludes end-of-life stage because significantly different demolition costs for the competing systems are not anticipated. Routine maintenance is also excluded. Maintenance costs are uncertain for a system that has yet to be implemented, like the HSR columns. However, an expert panel of bridge engineers (described in Valigura 2019) suggested that inspections of these columns could, eventually, be carried out with the same frequency and effort as conventional bridges. The seismic repair/failure stage encompasses the potential for seismic events during the design service life of the bridge of 75 years (AASHTO 2012). The costs and time of post-earthquake bridge repairs, but not pre-earthquake retrofit, are considered.

Upfront costs of construction and repair are sometimes referred to as *direct costs*. Time is used to indicate the number of days that it takes for the system to be constructed or repaired, and, particularly, the time that the traffic link (bridge) is closed due to on-site construction work. The economic impact of this closure time for bridge users constitutes *indirect costs*, which are calculated by converting time into dollars based on traffic characteristics of a given bridge.

3.2 Prototype Bridges

The LCCA is carried out for two prototype bridges (PB), described in Table 1. Each bridge defines a *functional unit* in LCCA terminology (Simonen 2014). Both represent modern seismically-designed bridges; PB1 is a narrow, but long, bridge, with a two-lane superstructure of five spans and single-column substructures, while PB2 is a suburban highway overcrossing, with a four-lane superstructure of two spans and a two-column pier substructure. Although PB1 and PB2 cannot completely characterize the entire class of RC bridges, they represent a range of characteristics of typical modern bridges in high seismic areas of California (FHWA 2015).

The baseline bridges with conventional columns are denoted PB1-C and PB2-C. PB1-C was designed by practicing engineers as a typical (hypothetical) code-designed bridge (Ketchum et al. 2004); PB2-C is an existing bridge in Orange, California. Design details are summarized in Valigura et al. (2019b).

The competing system bridges differ from the baseline bridges only in the columns, as indicated in Table 1. To design the HSR columns for these bridges, the requirements on HSR columns were to have the same height, and similar axial and flexural strength to their conventional column counterparts, and satisfy modern bridge safety/collapse requirements (Caltrans, 2010, 2013). As reported in Table 2, the HSR columns for PB1-H and PB2-H had circular hollow cross-sections, rocking joints at the top and bottom of each column, and two intermediate sliding joints (*i.e.,* three segments per column). The sliding and rocking joints were designed according to recommendations in Sideris et al. (2014b) and Salehi (2019). In particular, the sliding amplitude per joint was taken as 1% of clear column height, corresponding to a sliding of 6.3 cm (2.5 in) per joint, and a total maximum available sliding of 12.6 cm (5 in) per column. The 1% value is a design recommendation from previous research (Sideris et al. 2014b, Salehi 2019), as it can accommodate the displacements expected during design earthquake, and hence prevents damage to the column. The onset of sliding for PB1-H was at approximately 50% of the lateral strength capacity of the column, while for PB2-H, it was at 65%; in both cases, sliding preceded the onset of rocking. To achieve these capacities, PB-1H used a lubricated PTFE-on-PTFE interface (with coefficient of friction of 0.05), while dry PTFE-on-PTFE (with coefficient of friction of 0.1) was used for PB2-H. The sensitivity of results to the surface and its friction is discussed below.

Both versions of each PB have identical abutments, superstructure, and foundation. Of particular significance here is the gap between the superstructure and the shear keys and backwalls of the abutments. The bridge design for PB1 required a 5 cm (2 in) gap between the superstructure and both backwall or shear keys. In PB2, these gaps reduced to 2.5 cm (1 in) between the superstructure and backwall. The required backwall gaps are based on movement ratings of the superstructure (Caltrans, 1994) to accommodate possible movement of the structure due to temperature, prestressing, shrinkage, etc.; PB1 is longer than PB2, which results in a greater movement rating (and, hence, gap).

The design methodology produced some differences in periods between the bridges with HSR and conventional columns (Table 1), which may have some influence on displacement demands. However, unlike conventional bridges, the dynamic behavior of bridges with HSR columns is less dependent on initial period, and, hence, the difference in the initial periods in the design should not have significant effect on the results."

3.3 Assessment of Direct Construction and Repair Costs

Our assessment of direct costs accounts for differences in construction and repair costs that result from changes in the column design. For the baseline bridges, *i.e.* those with CIP columns, construction costs are determined based on material unit costs obtained from a Caltrans database of project bids (Caltrans 2017b). This database reports costs of materials that include material extraction and production, and transportation, labor to install/set the material, and equipment needed. Key values for each material have been previously reported (Valigura et al. 2019b).

The costs of the precast segments needed for the construction of the HSR columns are expected to be higher than the costs of CIP columns using the same amount of material due to precasting process and construction, which require tighter tolerances and skilled labor. Currently, there is no data on costs of precast segmental *column* construction in California. However, Caltrans (2019) reports estimated costs of precast elements. The authors analyzed Caltrans yearly cost estimates of precast and CIP girders and slabs since 2010, and found that, on average, construction of a precast element costs 1.25 times the construction of a CIP element of the same size. This multiplier accounts for different material needs and availability, construction techniques and their cost, and labor. This cost is somewhat lower than expert panel estimates in Valigura (2019), which indicated that panelists believed that initially the costs of the HSR system would be 1.5 times conventional column costs. However, the expert panel expected that the costs would be lower if the shapes were standardized, and their estimate also included the costs of interface materials, which are separately accounted for (as described below). Thus, the study adopts a 1.25 multiplier here, and the construction costs of the HSR column are calculated as:

$$HSR\ \ costs = 1.25 \times (conventional\ material\ costs) + interface\ material\ costs \quad (1)$$

where the conventional material costs include the structural concrete and steel reinforcement materials and related labor and equipment. The authors estimated interface materials costs, which also account for material, labor, and equipment, based on quotes obtained during construction of large-scale models (Salehi 2019; Valigura 2019), and the time and number of workers needed to attach the interface. These interface estimates contribute \$6,500 per column for PB1-H, and \$13,000 per column for PB2-H (Valigura 2019).

3.4 Assessment of Construction and Repair Time and Indirect Costs

Differences in construction and repair times between the baseline and competing system correspond to bridge (traffic link) closure. For our purposes, the construction time clock starts when the foundation block is cured and column construction commences. The clock ends when the column can support loads and construction can proceed above it, *i.e.,* the HSR column is posttensioned, or the concrete in the CIP column is cured sufficiently for construction to proceed above. This approach presumes, based on Abudayyeh et al. (2010), Caltrans (2017a) and other references, that columns are on the construction schedule's critical path and therefore, any change in construction time of the columns will directly affect the construction time of the entire bridge.

Construction of CIP columns involves construction of formwork and reinforcement cages, and pouring and curing the concrete. The construction time for each of these tasks was estimated based on schedules found in literature, prepared by professional estimators (Abudayyeh et al., 2010; Mackie et al., 2008). These data were used to develop Equation (2), which describes the number of days needed to construct CIP columns, T_C, based on the number of columns, n, and a mobilization multiplier, m:

$$T_C\ = round\ up\left(m \times 3 \times \frac{n}{8}\right) + round\ up\left(\frac{n}{4}\right) + 7\ \geq 9 \quad (2)$$

The first term represents the time to construct the formwork and place the reinforcement cage. The second term is the time for pouring concrete, which for four columns is expected to take one day. The third term accounts for the curing duration until the concrete acquires sufficient strength to withstand further loading; this curing time is taken as seven days (Caltrans, 2017a). The multiplier, m, is used because equipment mobilization time is relatively constant, regardless of the number of columns being constructed, and, hence, for a lower number of columns, it represents a larger portion of the construction time (Mackie et al., 2008). m is taken as 2 for four or fewer columns, and 1 for more than four columns. Equation (2) assumes that each of the two tasks starts on a new day, with a minimum total duration of nine days.

For HSR columns, construction times were estimated based on construction of the large-scale models described in Valigura (2019) and Salehi (2019). In the lab, the research team was able to place one segment in approximately 30 minutes, and posttensioning of a column could be also performed in under 30 minutes, thus, resulting in construction of three to four columns a day. These times are independent of the number of workers that can be dedicated to the task, because equipment (crane) availability governs. The study also used data from the Caltrans pilot bridge with precast columns (Caltrans, 2018), which showed assembly of two precast columns and cap beam was completed in under three hours. Accordingly, Equation (3) estimates construction times for HSR columns, T_H, which assumes that four HSR columns can be assembled and posttensioned in a single day with one crane, and adopts a lower limit of two days:

$$T_H = round\ up\left(\frac{n}{4}\right) \geq 2 \tag{3}$$

Bridge repair times are times of bridge closure. This time starts when the earthquake strikes and ends when the bridge can reopen for public use. The study assumes, consistent with Mackie et al. (2008), that repairs on different components of the bridge can be conducted in parallel, while repairs on a single component need to be performed in series. As a result, the total repair time for given shaking is governed by the component with the longest repair time. The details of the repair time calculation are described in the Seismic Performance Assessment section.

After estimating construction and/or repair times, the authors quantify the economic impacts of bridge closure during these times. These costs are borne by the traveling public and the surrounding economy. Werner et al. (2006) and Deco et al. (2013), among others, have presented methods to account for the economic impact of bridge closures, incorporating traffic flow analysis for bridge infrastructure. Caltrans has also developed their own framework, the California Life-Cycle Benefit/Cost Analysis Model (Caltrans, 2012), which uses California-specific information that can be used for estimating the economic impact of construction and repair time. The Caltrans method considers the redistribution of extra traffic to more than one detour based on traffic equilibrium. Our calculation assumes that 100% of trips will be rerouted. This assumption ignores opportunity costs from forgone trips (trips not taken due to bridge closure) (Moore et al., 2006), but accounts for the extra mileage and driver delays (Abudayyeh et al., 2010; Deco et al., 2013). The methodology follows closely the recommendations in Caltrans (2012). However, the methodology assumes that shortest detour as reported in FHWA (2015) is available (*i.e.,* undamaged in an earthquake), and do no traffic flow analysis. The details of the calculation of the indirect costs of bridge closure are provided in Valigura (2019), and correspond to $111,800 per day for PB1 and $13,300 per day for PB2 due to longer detour routes for PB1.

3.5 Seismic Performance Assessments

To obtain the seismic repair costs and times over the service life of the bridge, the PBEE framework is used (Deierlein et al., 2003).

3.5.1 Seismic Hazard

In terms of seismic hazard, the authors first assume both bridges are located in Orange, CA (33.781 degrees, -117.831 degrees) with site class D.

3.5.2 Nonlinear Dynamic Analysis

The assessment uses incremental dynamic analysis (Vamvatsikos and Cornell 2002) of the bridge models to determine the demands in the bridge, as a function of an intensity measure (IM). Here, spectral acceleration at the first-mode period of the bridge in the longitudinal direction is taken as the IM.

Our demand model is based on 2D models of each bridge in the longitudinal direction, with damage in transverse direction being estimated based on correlations observed in 3D models of bridges previously developed by the authors (Valigura et al. 2019b). The study here uses 2D model for both baseline and competing systems, because it is currently more computationally efficient analysis than 3D (specifically in the case of competing system). The longitudinal direction is used, because it allows for explicit modeling of abutments and superstructure unlike the transverse direction. Other studies have shown that abutments can significantly influence damage and repair estimates (Mackie et al. 2008; Valigura et al. 2019b). Simulation of PB1-C and PBC2-C in 2D (longitudinal direction) were validated against the results of 3D analysis presented in Valigura et al. (2019b), showing good agreement of in repair costs and their distribution between bridge elements.

The 2D models of each PB are modeled in *OpenSees* and consist of nonlinear models of bridge columns, linear elastic beam elements representing the superstructure, and springs modeling the abutment backwall and bearings, as shown in Figure 3. The superstructure is not expected to experience inelastic response. The abutments are simulated by springs representing the resistance of the bearings and backwall, calibrated to test data as described in Valigura et al. (2019b); the gap between the superstructure and backwall is also modeled. Foundation movement is captured using linear translation and rotational springs with values from Ketchum et al. (2004). More details about our bridge modeling are provided in Valigura et al. (2019b).

Each baseline CIP column is modeled with a single gradient inelastic (GI) flexibility-based beam column element (Salehi and Sideris 2017, 2018). The GI formulation has been shown to prevent strain localization during softening and provide numerical stability. The concrete material is modeled using Mander et al. (1988)'s model, while reinforcing steel uses a computationally-efficient material model that can capture both bar fracture and buckling (Valigura et al. 2019b). Rotational springs are added at the end of each column to represent bar slip.

HSR columns are modeled using a 2D HSR beam-column element proposed by Salehi et al. (2017). That model combines two components: a GI element that can effectively capture the rocking joint behavior through a compression only section, and a pressure-dependent hysteretic friction model to simulate joint sliding. The strands are modeled with a tension-only truss element. The interaction between the concrete segment and the unbonded PT strands is captured using gap elements. Salehi et al. (2017) showed that this model can adequately capture the fundamental HSR column response, including sliding-rocking interaction, tendon response, and interaction between the unbonded PT tendons and the duct and concrete segment, by comparing numerical simulations with experimental data from Sideris (2012).

Obviously, the 2D longitudinal analysis cannot predict the displacement and damage to abutment shear keys, which are damaged by bridge motion in the transverse direction. Valigura et al. (2019b) previously found that shear keys can contribute up to 20% of repair costs. Here, based on those results, correlations between damage states for backwall and shear keys were calculated, and used to predict damage in the (non-simulated) shear keys for both bridge systems.

The study adopts the FEMA P-695 far field ground motions to represent seismic excitation (FEMA, 2009). These ground motions are an appropriate choice for a typical high seismic site in California to provide a baseline comparison between bridges.

3.5.3 Damage States and Repair Strategies for Bridge Elements

A large body of research has been conducted on damage and repair assessment of conventional RC bridges, especially to their columns, *e.g.*, Fakharifar et al. (2016), Vosooghi and Saiidi (2013). The authors adopt the damage states and repair strategies defined in Valigura et al. (2019b) for conventional columns and all other non-HSR components. Conventional columns are assumed to be repaired with carbon fiber reinforced polymer jackets if jacketing is needed.

Valigura (2019) investigated damage states and repair strategies for HSR columns, using large-scale experiments and a panel of bridge experts. These damage states include residual drift and segment damage states. Segment damage states involve primarily damage to rocking joints, ranging from minor spalling to crushing of core concrete. The residual drift damage states depend on two effects, joint sliding, which can be restored by hydraulic or mechanical means as described below, and concrete damage (spalling and/or crushing) in the vicinity of the rocking joint, which is permanent. All damages states are determined at the element level, based on either stress-strain response in critical section (columns), or displacements of the elements (abutments). The collapse is based on structural level behavior and defined as a loss of stability, or unseating of superstructure (Valigura et al. 2019b). The repair method for each damage state is shown in Table 3.

3.5.4 Repair Costs and Time for Bridge Elements

The unit costs of all repair materials and processes for conventional elements are estimated from the same Caltrans (2017) data used for determining upfront construction costs, with details reported in Valigura et al. (2019b).

For the conventional columns (baseline system) and other conventional elements (both baseline and competing systems), repair times are estimated based on reported values for each damage state and each task in the repair process from Mackie et al. (2008), with median values shown in Tables 4 and 5. The repair time for each DS is determined by the time required for each individual task in the repair process; for example, column DS5 would involve temporary shoring, excavation around the column heel, patching of spalled and crushed concrete, applying and curing the CFRP jacket, backfill around the column, and removing the temporary shoring. The repair times are taken from Mackie et al. (2008). When appropriate, the repair times were scaled to represent increased labor based on the size of the element. Valigura (2019) provides the breakdown for each element and DS.

The repair strategies introduced for HSR columns in Valigura (2019) were recommended by the aforementioned panel of bridge engineering experts. The repair costs for the HSR column are determined based on the amount of each material needed for the repair. The columns do not require any special materials, except for the interface, the costs of which have been previously defined; the rest of the material unit costs are provided in Valigura et al. (2019b). In addition, hydraulic jacks can be used to restore the residual drifts from joint sliding. In this repair scenario, the superstructure would not have to be lifted, because the coefficient of friction is low enough for jack to pull the structure back. The hydraulic jack would bear against lower segment and pull the upper segment into its place. As the cost of jacks are not separately provided in the data set employed here (Caltrans, 2017b), the authors conservatively take the costs of these jacks as equal to the cost of temporary support.

Repair times for each HSR column DS are determined from the tasks involved in the process of repair, with the results shown in Table 6; Valigura (2019) provides a breakdown of tasks/times for each DS. For most of the DSs, the repair tasks are similar to tasks for the baseline CIP columns repaired with CFRP jacket, except for re-tensioning or replacement of the tendons. Re-tensioning of tendons would require the tendons to extend about 1 ft. above the anchorage at the top of the cap beam and be housed in a box to allow for access after earthquake. In the case that the tendons would need to be replaced, additional detail in the foundation block in form of 180-degree turn is needed to allow for access (e.g., SEAOC 2016). Table 6 indicates that the replacement time of the HSR column is estimated to be in fact shorter than repair time of DS3; this shorter time is because the precast segments only need to be assembled on-site, which takes less time than patching spalled concrete, and applying and curing CFRP.

Permitting is assumed to be required if temporary shoring and/or repair to structural damage of columns (DS3 and higher) is needed (indicated by * in Tables 4-6). The length of permitting process is estimated as 30 days (Mackie et al., 2008).

3.5.5 Repair Cost and Time Vulnerability Curves and Life-Cycle Impacts

Repair costs are calculated as a summation of the repair costs for each element. The study assumes repair costs are performed in parallel on different components, such that the total repair time is taken as the maximum of column, abutment (sum of times to repair bearing, shear keys, and backwall), and deck repair times. This process produces repair cost and repair time vulnerability curves, which represent the relationship between the IM and repair costs or time.

To calculate the total cost and time in the bridge's seismic repair/failure stage of its life-cycle, the methodology determines annualized losses or days lost to repair by convolving the repair cost and time vulnerability curves with the site seismic hazard curve. Over the bridge's 75 year lifespan, the seismic repair costs and economic value of seismic repair time are calculated as present value (in 2017 dollars) from the annualized losses based on an annual discount rate of 3.0%

(Zerbe and Falit-Baiamonte, 2001). The life-cycle repair time impacts are determined by summing the annualized days lost to repair.

3.6 Treatment of Uncertainty

The LCCA considers uncertainty in each stage of the assessment. In the construction stage, the material unit costs are assumed to follow the lognormal distribution (FEMA 2012), with distribution values for all materials provided in Valigura et al. (2019b). These distributions account for both the variability in the material quantity estimate (because they are based on material quantity in the bid, not on actual quantity used) and variability in unit material cost (because they are based on bids from different bidders). No correlations are assumed between different material costs. Although material cost variability may be lower for precast construction, because it is a more controlled process, these data are not present in our data set to verify. In addition, because the use of column precast construction is very limited in high seismic areas, the cost multiplier for precast construction of 1.25 is treated probabilistically, and assumed to be uniformly distributed between 1.15 and 1.35. The dispersion in interface material costs is assumed as a relatively small lognormal standard deviation of 0.4; the main cost of the interface comes from PTFE material which is produced by only a few manufacturers.

The construction time estimates are assumed to be normally distributed about the mean reported in Equations (2) and (3). The study adopts a coefficient of variation of 0.3 for both CIP and HSR columns; this coefficient of variation is half of the variability defined in Hazus (FEMA, 2017) for repair/restoration time for major damage, because new construction is a more controlled process than repairs. The lower bound on the time estimates is enforced in the Monte Carlo simulation.

The cost and time assessment in the seismic repair/failure stage accounts for motion-to-motion variability, uncertainty in the onset of damage states, and variation of the unit material cost (Valigura et al. 2019b). Repair times are assumed to follow lognormal distributions with the dispersion values being estimated based on the standard deviation of repair/restoration times provided in Hazus (FEMA 2017). For repairs, the entire dispersion from Hazus is used, because the definition of repair time here is equivalent with Hazus' definition of restorations time, as reported in Tables 4-6. The economic impact of repair and construction times is calculated deterministically because of the lack of available data to quantify underlying uncertainties.

Uncertainty is propagated through Monte Carlo simulation with 5000 realizations of construction costs and times, which are treated independently from each other; 5000 realizations is sufficient to produce results that are not sensitive to the number of realizations. For the seismic repair/failure stage, 5000 realizations of correlated demand parameters are generated for each IM. The damage state for each element depends on the realization of demands in the element, as well as the randomly generated damage state thresholds. From the damage state, a realization of repair costs and repair time is generated from their respective distributions. For a given realization, the methodology assumes perfect correlation between repair costs (or time) of the CIP and HSR columns. This assumption is motivated by the almost identical types of repair actions of the two systems. As a result, if the same contractor was hired to repair either system in response to a given earthquake, the bids would be correlated above or below the median. The authors assume the random variables associated with repair costs and repair time are independent of each other. Construction costs and times are assumed to be uncorrelated from repair costs and time.

4. Results

4.1 Seismic Performance of Prototype Bridges

The seismic performance of the bridge systems is assessed first through longitudinal displacements, and repair cost and time vulnerability curves. Figure 4 compares the mean displacements of the superstructure, with respect to the shaking intensity. Results for both PB1 and PB2 show that for IMs up to about 70% of the design level, the displacements of the competing system and baseline system bridges are similar, with slightly higher displacements for the bridges with HSR columns, due to sliding. Sliding initiates at 20% of the design IM (Figure 4). At larger IMs, the displacements of the baseline bridges exceed that of the HSR competing system. In this regime of excitation, the HSR columns' joint sliding provides substantial additional damping in the system, limiting the displacement demands relative to the baseline columns.

These displacement demands significantly influence the vulnerability curves. Figure 5 presents the repair costs, and their deaggregation to show contributing components. Figure 6 provides the same information for repair times. For both PB1 and PB2, the HSR columns behave as designed, and limit the damage to columns (and, as a result, associated repair costs and time). However, because of the HSR system's larger displacement demands at lower IMs, additional damage occurs to the abutments in this range of response, compared to the baseline system. As a result, the abutments account for almost all repair costs and time for the HSR system while, for the baseline system, the repair costs and time are distributed among various elements. Abutment damage is more significant for PB2 than PB1 because of the smaller gaps between backwall and superstructure, and the larger abutments for PB2. In both cases, these effects produce generally lower repair costs and times for the competing HSR system, but there is a smaller difference between the systems for PB2, due to more abutment damage.

4.2 Life-Cycle Cost Assessment

For each PB, the results of the LCCA are presented first considering only the direct costs, taking the direct construction and direct seismic repair costs of the competing system and subtracting the corresponding costs for the baseline system for each life-cycle stage. Thus, positive values indicate that the competing HSR system has economic (direct) benefits compared to the baseline system, whereas the opposite is true for negative values.

As shown in Figure 7, the direct costs in the construction stage are higher for PB1-H and PB2-H as compared to PB1-C and PB2-C, respectively. This difference is due to the greater costs of precast processes, post-tensioning, and the sliding interfaces of the HSR columns compared to conventional columns. However, as reported in Figure 5a, PB1-H has lower or similar earthquake repair costs (as a function of IM) compared to PB1-C, producing overall benefits on the side of the competing (HSR) system in the seismic repair/failure stage in Figure 7a. These benefits outweigh the benefits of the baseline system from the construction stage, such that, overall, over the lifespan of the bridge, HSR column construction has life-cycle benefits equivalent to 1.3% of the replacement cost of the baseline system for PB1 from direct costs alone. However, recalling from Figure 5b that the repair costs of PB2-H are slightly higher at lower IM levels than PB2-C, for this bridge, the benefits in the seismic repair/failure stage are not sufficient to outweigh the higher construction costs in Figure 7b. As a result, the life-cycle benefits for PB2 from direct costs, correspond to 0.6% of the replacement cost of the baseline system, in favor of the baseline system.

Figures 7 through 9 also show that the dispersion does not change the outcome of the results in terms of which system is more beneficial, but it does affect the magnitude of benefits. Focusing on the total benefits in Figure 9, the uncertainty tends to increase the "tail" in the direction of higher benefits for the HSR system.

4.3 Life-Cycle Time Assessment

The time assessment here presents the benefits of either system in terms of time (days) saved during construction and seismic repair/failure stages (top panel of Figure 8) and this time's economic impacts, *i.e.,* indirect costs (bottom panel of Figure 8). In the construction phase, the competing system has benefits relative to the baseline system, because of the shorter construction time needed for HSR columns, for which, only the assembly process happens on-site.

For PB1, PB1-H has slightly shorter seismic repair times at lower IMs, and more significantly shorter repair times than PB1-C for higher IMs (Figure 6a). These benefits of the HSR system, combined with time benefits during construction stage, make PB1-H more promising than PB1-C when both construction and seismic repair/failure stages are combined, with a mean of 78 closure days fewer over the entire life-cycle of the bridge. In economic terms, this corresponds to indirect economic benefits of 130% of the baseline bridge replacement cost. This favorable assessment of the competing HSR system results from the relatively large time savings of the HSR bridge, and also from the significant costs of closure of $111,800/day for PB1. Results of PB2 follow the same logic; however, due to the vulnerability time curves of the baseline and competing bridges being more similar, the total life-cycle time benefits of the competing system are 32 days. In addition, the time effect of closure is only $13,300/day for PB2, such that life-cycle indirect benefits of the competing (HSR) system are 5% of the baseline bridge replacement cost.

4.4 Life-Cycle Assessment of Total Costs

The total costs include both direct and indirect costs during both construction and seismic repair/failure stages, providing the life-cycle assessment of the benefits of the two systems with results shown in Figure 9. The competing HSR system has greater total life-cycle benefits relative to the baseline system for both PB1 and PB2. The construction stage benefits stem from the economic impacts of reduced construction time, which outweigh the extra direct costs of the HSR column construction in this stage. In the seismic repair/failure stage, the benefits come from lower repair costs and decreased repair times due to the superior seismic performance of the HSR system.

The total life-cycle benefits of the competing system for a given location are 135% and 4% of the replacement costs of the baseline system for PB1-H and PB2-H, respectively. In other words, construction of the HSR system in lieu of the conventional system would save 135% and 4% of the replacement costs of the system over its lifetime. The big differences in the outcome for PB1 and PB2 can be tracked to PB1-H's much improved seismic performance with respect to its baseline counterpart and the significant economic impact of bridge closure (due to traffic characteristics of the bridge), producing large indirect benefits.

4.5 Sensitivity Analysis

In this section, a sensitivity analysis was conducted to explore how characteristics of the site and bridge, or our assumptions made in conducting the study, may impact the principal finding: that bridges with HSR columns have life-cycle benefits compared to conventional bridge systems. The variables examined in the sensitivity analysis are those that are most uncertain, or may have a significant impact on the assessment for construction or seismic repair/failure stages or both, namely:

- Site seismic hazard: We examined PB1 and PB2 bridges in both baseline and competing system configuration for 26 western U.S. seismic locations and sites classes B and D to represent the range of common site classes for high seismic areas in California (Wills et al. 2000). Locations of these additional sites are defined in Valigura et al. (2019a).
- Interface material costs: Costs were varied to account for possible use of different materials beyond those tested by the authors. This variation considered cost estimates much higher than the expected value to avoid unintended bias in favor of the HSR system.
- Cost multiplier on precast costs: The multiplier is taken as 1.25 for most of the analyses in the paper, but is increased up to 2.5 in the sensitivity analysis to account for potential much higher costs of the innovative HSR columns during early implementation of the system.
- Construction time for conventional and HSR columns: The assumed construction times were intentionally pessimistic for the HSR columns. However, to explore a worst-case scenario, as well as more realistic times, the construction time difference between conventional and HSR columns was varied.
- HSR column replacement time: The HSR column post-earthquake replacement time was varied to account for potential slower replacement time for the HSR system, considering the case where, for example, a contractor would not be familiar with the system.
- Bridge daily traffic and detour length: Bridge daily traffic varies over time, and among different similar bridges in California. In addition, our estimates of detour length are probably optimistically short, as in an earthquake, the shortest alternate route may not be available.

The range of the variables considered is provided in Figures 10 and 11. Each variable is varied individually.

The results for variation in seismic hazard are shown in Figure 10; the rest of the results are shown in Figure 11 where "default" indicates the result presented previously. These figures show that, regardless of the variable examined and the bridge of interest, the benefits are on the side of the competing, HSR, system with benefits greater than zero. The only exception is if the precast cost multiplier is 2.5 times for PB2, in which case PB2-C and PB2-H are essentially cost equivalent. The most influential variables were daily traffic and detour length, underlining the conclusions that the HSR columns are most suitable for important infrastructure links. These findings also indicate potential situations in which the HSR system may not be as beneficial, specifically for bridges with low traffic and for bridges where general precast systems would result in significantly larger initial costs than cast-in-place systems. The results also show that, the greater the seismic hazard, the greater the benefit; the HSR system generally had better seismic performance (and, therefore, lower repair costs and time) than the baseline system for the same intensity of shaking, and, thus, with higher probability of these shakings occurring at sites with greater seismic hazard, the difference between seismic repair/failure contributions to direct and indirect costs of the competing and baseline systems increase. The results also show the largest benefits for the competing HSR system in Los Angeles and the San Francisco Bay area, as compared to Seattle because Seattle has relatively lower frequency of low intensity shakings. The benefits of HSR system in regions with moderate seismicity may not be as pronounced and further research would be required to quantify them more accurately on a case-by-case basis.

In addition, a central limitation is benefits that could not be quantified or considered in the assessment. Here, there are unquantified benefits associated with the shorter construction/repair times of HSR columns. These include improved road safety, reduced noise, and reduced health and environmental impacts for surrounding communities (Culmo 2011). Public safety impacts associated with avoiding bridge failure were also not considered. These additional considerations further amplify the differences between the baseline and competing systems, each weighting the assessment even more heavily in favor of the bridges with the HSR column system. In addition, the study assumed that only the columns differ between the two systems. However, bridges with ABC-compatible precast columns, like HSR columns, would likely also employ ABC precast superstructure elements. Compared to a fully CIP conventional baseline system, this system would have even more benefits in terms of construction and repair times.

4.6 Implications of Results for Design of Bridges with HSR Columns

In general, the results reveal that the competing system is economically beneficial (compared to the baseline system) even when only the construction stage is considered. However, the more significant benefits come from the HSR system's superior seismic performance; as a result, as a bridge site's seismic hazard increases, so do the benefits of bridges with HSR columns.

One of the key design variables for HSR columns is the lateral force at which sliding initiates, which depends on the coefficient of friction of the interface. If sliding initiates too early, the displacement demands on the columns are large at low intensity shakings; if sliding initiates too late, it may be preceded by significant rocking response, which is more damaging. Our initial design aimed at an onset of sliding between 35% and 65% of the capacity of the column. For PB2-H, with interface coefficients of friction of 0.05, the sliding initiated at approximately 35% of the ultimate column base shear strength, which was at the lower end of the target range. However, a preliminary seismic assessment revealed that this lower onset of sliding produced excessively high displacements at low IMs, as shown in Figure 12a. This exposed an incompatibility in the design philosophy in that sliding was allowed in the HSR column, but the abutment (gap) design had not been altered to accommodate larger demands. As a result, for this preliminary design of PB2-H, repair costs and repair times were large (Figure 12b). Recognizing that abutment and column displacement compatibility was necessary, the authors redesigned PB2-H with a higher coefficient of friction and sliding onset at about 65% of the ultimate column strength (these are the results the study have heretofore presented).

This assessment therefore informs recommendations for future design of HSR columns. In particular, the sensitivity of repair costs to the more frequent, low intensity events implies that the onset of sliding should be based as a fraction of the design base shear demand. From the results shown in Figure 12, the authors recommend that the onset of sliding not occur until at least 20% of the design intensity. This requirement should limit the sliding displacement to acceptable levels during low intensity shakings, and prevent extensive damage to abutments. Furthermore, this study suggests the need to adopt compatibility requirements between the column's sliding amplitude and the gap between superstructure and abutments. For example, base isolated bridges must have sufficient gap between superstructure and abutments to accommodate displacement demands from the design earthquake (Buckle et al. 2006). By applying the same requirement to bridges with HSR columns, the HSR system benefits would further increase compared to those reported here because of the reduced damage to the abutments. This idea was also recommended by the expert panel of bridge engineers convened by Valigura (2019). This could be further beneficial for HSR bridges, because the sliding is designed to accommodate 1% of a drift (corresponding roughly to design earthquake displacement). If the abutments could sustain this drift without any or only with limited damage, the seismic repair time and costs would further decrease.

An additional factor requiring more consideration is the friction coefficient. First, the breakaway friction, which for PTFE may be higher than coefficients of kinetic and static friction (Goli, 2019), could prevent sliding at low shaking levels. If too high, this friction could potentially eliminate the sliding and its beneficial impacts. Deterioration of the sliding surface could potentially have similar effect. Neither of these effects was considered in the study, because these effects are assumed to be avoided by appropriate material design/specification. Nevertheless, after required research on breakaway friction is performed, it should be incorporated into the friction model for future LCCA studies.

5. Summary and Conclusions

This paper applies LCCA to compare different design strategies for bridges in high seismic areas. The assessment considers bridge systems with conventional and HSR RC columns; HSR columns are compatible with ABC. The assessment includes two stages of a bridge's life cycle: the construction stage, and the seismic damage/repair stage. The assessment employs the PBEE framework to determine earthquake-induced repair costs and times associated with the seismic repair/failure stage. The LCCA encompasses direct costs and indirect costs, with the latter being associated with traffic impacts of bridge closure during construction/repair times. The assessment is applied to two prototype bridges, each designed with conventional and with HSR columns.

The results of the seismic repair/failure life-cycle stage show the benefits of the HSR system in terms of seismic performance. For both bridges, the seismic repair costs and time are governed by the performance at low-to-medium shaking intensities. For these intensities of shaking, the use of HSR columns eliminates column damage. This results in lower repair costs and times for bridges with HSR columns than for bridges with conventional columns under the same intensity of shaking. These effects are most significant for bridges where columns, rather than abutments, contribute significantly to the damage.

The findings of this study suggest that bridge systems with HSR columns have economic benefits in both life-cycle stages due to their quick construction and low damage potential. Bridges with HSR columns would be especially beneficial for important traffic links (with high traffic volumes on the bridge) and for traffic links with long detour options. This is because the most significant contributor to the benefits come from indirect costs associated with bridge closure in both construction and seismic repair/failure stages, which is highly dependent on traffic volume and detour length. However, as shown in the sensitivity study, there are potential bridge characteristics combinations that may result in HSR columns not being beneficial, or not as beneficial. As an example, a link with very low daily traffic, relatively short detour, and high initial costs of precasting (with respect to casting-in-place) would likely result in benefits on the side of cast-in-place columns. In such cases, a site-specific life-cycle cost assessment may help to guide the system choice. Furthermore, the benefits of HSR columns in sites with moderate seismicity may not be as significant.

Although this study focuses on HSR columns, one possible ABC column system, the findings suggest overall an advantage to use of ABC for bridge substructures. In particular, on highly trafficked routes, there are major economic benefits from reducing construction and repair time alone. These benefits are even more increased if the ABC system, like HSR, is not only quick to construct, but also has lower damage potential than the conventional alternative. This low damageability is most critical in high seismic areas. Our results show that for a broad range of bridge characteristics, these characteristics show advantages to using a new ABC system, even if costs of construction are as much as double the conventional system. More work is needed to more precisely quantify these observations for other ABC column systems.

Acknowledgments

This research was funded by the National Science Foundation (NSF) under Award No. CMMI 1538585/1748031. The authors appreciate suggestions on the manuscript from Drs. Sarah Welsh-Huggins, Jamie Padgett, and Keith Porter, as well as the help of Mr. Adan Camacho and Dr. Mohammad Salehi.

References

AASHTO. (2012). *AASHTO LRFD Bridge Design Specifications* (6th ed.). Washington, D. C.: American Association of State Highway and Transportation Officials.

Abudayyeh, O., Cai, H., Mellema, B., & Yehia, S. (2010). Quantifying Time and User Cost Savings for Rapid Bridge Construction Technique. *Journal of Transportation Research Board*, (2151), 11–20.

Buckle, I. G., Constantionou, M., Dicleli, M., & Ghasemi, H. (2006). *Seismic Isolation of Highway Bridges* (No. MCEER-06-SP07; p. 171).

Caltrans. (1994, September). *Memo to Designers 7-10*. California Department of Transportation.

Caltrans. (2008). *Accelerated Bridge Construction Application in California—A "Lessons Learned" Report* (p. 55). Sacramento, CA: California Department of Transportation.

Caltrans. (2010, July). *Memo to Designers 20-1*. California Department of Transportation.

Caltrans. (2012). *California Life-Cycle Benefit/Cost Analysis Model (Cal-B/C)—Volume 3*. California Department of Transportation.

Caltrans. (2013). *Caltrans Seismic Design Criteria Version 1.7*. Sacramento, CA: California Department of Transportation.

Caltrans. (2017). Contract Cost Data. Retrieved September 14, 2017, from http://sv08data.dot.ca.gov/contractcost/index.php

Caltrans. (2018, January). *Laurel Street Overcrossing*. Retrieved from http://www.dot.ca.gov/hq/esc/osfp/acec-des/2018-01-26-abc-laurel-des-acec.pdf

Caltrans. (2019). Cost Estimates Branch. Retrieved March 20, 2019, from http://www.dot.ca.gov/hq/esc/estimates/

Culmo, M. P. (2011). *Accelerated Bridge Construction—Experience in Design, Fabrication and Erection of Prefabricated Bridge Elements and Systems* (No. FHWA-HIF-12-013). Federal Highway Administration.

Deco, A., Bocchini, P., & Frangopol, D. M. (2013). A Probabilistic Approach for the Prediction of Seismic Resilience of Bridges. *Earthquake Engineering and Structural Dynamics*, *42*(10), 1469–1487.

Deierlein, G. G., Krawinkler, H., & Cornell, C. A. (2003). A Framework for Performance-Based Earthquake Engineering. *Pacific Conference on Earthquake Engineering*, 1–8. Christchurch, New Zealand: New Zealand Society for Earthquake Engineering.

Fakharifar, M., Chen, G., Chenglin, W., Shamsabadi, A., ElGawady, M. A., & Dalvand, A. (2016). Rapid Repair of Earthquake-Damaged RC Columns with Prestressed Steel Jackets. *Journal of Bridge Engineering*, *21*(4), 04015075.

FEMA. (2009). *Quantification of Building Seismic Performance Factors* (No. FEMA P695). Washington, DC: Federal Emergency Management Agency.

FEMA. (2012). *Seismic Performance Assessment of Buildings Volume 1—Methodology* (No. FEMA P-58-1). Washington, DC: Federal Emergency Management Agency.

FEMA. (2017). *Hazus—MH 2.1: Technical Manual*. Washington, DC: Federal Emergency Management Agency.

FHWA. (2015). National Bridge Inventory. Retrieved October 15, 2016, from https://www.fhwa.dot.gov/bridge/nbi/ascii.cfm

Frangopol, D. M., & Liu, M. (2007). Maintenance and Management of Civil Infrastructure Based on Condition, Safety, Optimization, and Life-Cycle Cost. *Structure and Infrastructure Engineering*, *3*(1), 29–41.

He, R., Yang, Y., & Sneed, L. H. (2015). Seismic Repair of Reinforced Concrete Bridge Columns: Review of Research Findings. *Journal of Bridge Engineering*, *20*(12), 04015015.

Hewes, J. T. (2007). Seismic Tests on Precast Segmental Concrete Columns with Unbonded Tendons. *Bridge Structures*, *3*(3–4), 215–227.

Ketchum, M., Chang, V., & Shantz, T. (2004). *Influence of Design Ground Motion Level on Highway Bridge Costs* (No. 6D01). Pacific Earthquake Engineering Research Center.

Lee, W. K., & Billington, S. L. (2011). Performance-Based Earthquake Engineering Assessment of a Self-Centering, Post-Tensioned Concrete Bridge System. *Earthquake Engineering and Structural Dynamics*, *40*(8), 887–902.

Lehman, D. E., & Roeder, C. W. (2012). Foundation Connections for Circular Concrete-Filled Tubes. *Journal of Constructional Steel Research*, *78*, 212–225.

Mackie, K. R., & Stojadinovic, B. (2005). *Fragility Basis for California Highway Overpass Bridge Seismic Decision Making* (No. PEER 2005/12). Pacific Earthquake Engineering Research Center.

Mackie, K. R., Wong, J.-M., & Stojadinovic, B. (2008). *Integrated Probabilistic Performance-Based Evaluation of Benchmark Reinforced Concrete Bridges* (No. PEER 2007/09; p. 162). Pacific Earthquake Engineering Research Center.

Mander, J. B., Priestley, M. J. N., & Park, R. (1988). Theoretical Stress-Strain Model for Confined Concrete. *Journal of Structural Engineering*, *114*(8), 1804–1826.

Matsumoto, E. E., Waggoner, M. C., Kreger, M. E., Vogel, J., & Wolf, L. (2008). Development of a Precast Concrete Bent-Cap System. *PCI Journal*, *53*(3), 74–99.

Moore, J. E., Cho, S., Fan, Y. Y., & Werner, S. (2006). *Quantifying Economic Losses from Travel Forgone Following a Large Metropolitan Earthquake* (No. PEER 2006/09). Pacific Earthquake Engineering Research Center.

Motaref, S., Saiidi, M. S., & Sanders, D. H. (2011). *Seismic Response of Precast Columns with Energy Dissipating Joints* (No. CCEER-11-01; p. 707). Center for Civil Engineering Earthquake Research, University of Nevada.

Ou, Y.-C., Tsai, M.-S., Chang, K.-C., & Lee, G. C. (2010). Cyclic Behavior of Precast Segmental Concrete Bridge Columns with High Performance or Conventional Steel Reinforcing Bars as Energy Dissipation Bars. *Earthquake Engineering and Structural Dynamics*, *39*(11), 1181–1198.

Restrepo, J. I., Tobolski, M. J., & Matsumoto, E. E. (2011). *Development of a Precast Bent Cap System for Seismic Regions* (No. NCHRP Report 681; p. 106). National Cooperative Highway Research Program.

Sakai, J., & Mahin, S. A. (2004). *Analytical Investigations of New Methods for Reducing Residual Displacement of Reinforced Concrete Bridge Columns* (No. PEER 2004/02; p. 291). Berkeley, CA: Pacific Earthquake Engineering Research Center.

Salehi, M. (2019). *Nonlinear Modeling, Dynamic Analysis, and Experimental Testing of Hybrid Sliding-Rocking Bridges* (PhD). Texas A&M University, College Station, TX.

Salehi, M., & Sideris, P. (2017). Refined Gradient Inelastic Flexibility-Based Formulation for Members Subjected to Arbitrary Loading. *Journal of Engineering Mechanics*, *143*(9), 04017090.

Salehi, M., & Sideris, P. (2018). A Finite-Strain Gradient-Inelastic Beam Theory and a Correcponding Force-Based Frame Element Formulation. *International Journal for Numerical Methods in Engineering*, *116*(6), 380–411.

Salehi, M., Sideris, P., & Liel, A. B. (2017). Numerical Simulation of Hybrid Sliding-Rocking Columns Subjected to Earthquake Excitation. *Journal of Structural Engineering*, *143*(11), 04017149.

SEAOC (2016). Excellence in Structural Engineering Awards - Comstock Graduate Student Housing. <https://cdn.ymaws.com/www.seaoc.org/resource/resmgr/docs/EISE2016/4a-displayboard-comstock.pdf>

Sideris, P. (2012). *Seismic Analysis and Design of Precast Concrete Segmental Bridges* (PhD). University of Buffalo, State University of New York.

Sideris, P., Aref, A. J., & Filiatrault, A. (2014a). Large-Scale Testing of a Hybrid Sliding-Rocking Posttensioned Segmental Bridge System. *Journal of Structural Engineering*, *140*(6), 04014025.

Sideris, P., Aref, A. J., & Filiatrault, A. (2014b). Quasi-Static Cyclic Testing of a Large-Scale Hybrid Sliding-Rocking Segmental Column with Slip-Dominant Joints. *Journal of Bridge Engineering*, *19*(10), 04014036.

Sideris, P., Aref, A. J., & Filiatrault, A. (2015). Experimental Seismic Performance of a Hybrid Sliding-Rocking Bridge for Various Specimen Configurations and Seismic Loading Conditions. *Journal of Bridge Engineering*, *20*(11), 04015009.

Simonen, K. (2014). *Life Cycle Assessment* (1st ed.). Routhledge.

Tazarv, M., & Saiidi, M. S. (2013). Analytical Studies of the Seismic Performance of a Full-Scale SMA-Reinforced Bridge Column. *International Journal of Bridge Engineering*, *1*(1), 37–50.

Tazarv, M., & Saiidi, M. S. (2014). *Next Generation of Bridge Columns for Accelerated Bridge Construction in High Seismic Zones* (No. UNR/CCEER 14-06). Department of Civil and Environmental Engineering, University of Nevada, Reno.

Valigura, J. (2019). *Seismic Repair and Loss Assessment of Bridges with Hynrid Sliding-Rocking Columns* (PhD). University of Colorado, Boulder, Boulder, CO.

Valigura, J., Liel, A. B., & Sideris, P. (2019a). Consideration of Post-Repair Performance in Seismic Loss Assessment of Structures. *13th International Conference on Applications of Statistics and Probability in Civil Engineering, ICASP13*. Seoul, South Korea.

Valigura, J., Liel, A. B., & Sideris, P. (2019b). Risk-Based Assessment of Seismic Repair Costs for Reinforced Concrete Bridges, Considering Competing Repair Strategies. *Journal of Bridge Engineering*, *24*(11).

Vamvatsikos, D., & Cornell, C. A. (2002). Incremental Dynamic Analysis. *Earthquake Engineering and Structural Dynamics*, *31*, 491–514.

Vosooghi, A., & Saiidi, M. S. (2013). Shake-Table Studies of Repaired Reinforced Concrete Bridge Columns Using Carbon Fiber-Reinforced Polymer Fabrics. *ACI Structural Journal*, *110*(1), 105–114.

Werner, S. D., Taylor, C. E., Cho, S., Lavoie, J.-P., Huyck, C., Eitzel, C., … Eguchi, R. T. (2006). *REDARS 2: Methodology and Software for Seismic Risk Analysis of Highway Systems* (No. MCEER-06-SP08).

Wills, C. J., Petersen, M., Bryant, W. A., Reichle, M., Saucedo, G. J., Tan, S., … Treiman, J. (2000). A Site-Conditions Map for California Based on Geology and Shear-Wave Velocity. *Bulletin of the Seismological Society of America*, *90*(6B), S187–S208.

WSDOT. (2009). *WSDOT Strategic Plan Accelerated Bridge Construction (ABC)*. Washington State Department of Transportation.

WSDOT. (2018). *Bridge Design Manual (LRFD)*. Washington State Department of Transportation.

Yang, C., DesRoches, R., & Padgett, J. (2009). Fragility Curves for a Typical California Box Girder Bridge. *Technical Council on Lifeline Earthquake Engineering Conference*. Oakland, California.

Zerbe, R. O., & Falit-Baiamonte, A. (2001). *The Use of Benefit-Cost Analysis for Evaluation of Performance-Based Earthquake Engineering Decisions* (No. PEER 2002/06; p. 83). University of Washington: Pacific Earthquake Engineering Research Center.

Tables

Table 1. Comparison of baseline and competing column systems for PB1 and PB2.

	PB1-C	PB1-H	PB2-C	PB2-H
Fundamental period of the bridge in transverse direction (s)	1.32	1.30	0.89	0.81
Fundamental period of the bridge in longitudinal direction (s)	0.90	0.85	0.85	0.72
Number of spans	5		2	
Number of columns	4		2	
Number of traffic lanes (each direction)	1		2	
Total length (m) [ft]	140 [460]		94 [310]	
Column height (m) [ft]	6.7 [22]			
Column gravity load demand to capacity ratio (%)*	8	9	7	6
Column moment strength (kN.m) [kip.ft]	4560 [3370]	4950 [3650]	23000 [17000]	23900 [17625]

* Calculated as unfactored dead load over nominal capacity of the column. PT forces are excluded.

Table 2. HSR column properties for PB1-H and PB2-H.

	PB1-H	PB2-H
Segment height bottom/middle/top (m) [ft]	2.1/1.5/3.1 [7/5/10]	2.4/1.9/2.4 [8/6/8]
Diameter external/internal (cm) [in]	168/107 [66/42]	229/137 [90/54]
Concrete strength (MPa) [ksi]	36.5 [5.3]	48.2 [7.0]*
Number of tendons	24	88
Diameter of tendons (cm) [in]	1.5 [0.6]	1.8 [0.7]
Yield strength of tendons (MPa) [ksi]	1860 [270]	
Sliding amplitude per joint (cm) [in]	6.4 [2.5]	
Volumetric ratio of longitudinal reinforcement (%)	1.0	2.0

* High strength concrete was used here to increase moment capacity without further increasing the external diameter

Table 3. HSR column damage states and repair strategies.

DS	Qualitative description	Repair strategy
Segment damage states		
DS 1	Open cracks	Epoxy injections
DS 2	Spalling at the rocking joint	CFRP or light-gage steel jacket (1 MPa [150 psi]) Re-tension the tendons
DS 3	Extensive spalling at the rocking joint with visible reinforcement; Tendon yielding	CFRP or light-gage steel jacket (2 MPa [300 psi]) Replace the tendons
DS 4	Extensive spalling at the rocking joint with crushed concrete in the core Tendon fracture	Replace the column
Residual drift damage states		
DS R1	Small sliding residual drifts	No repair
DS R1	Sliding residual drifts	Re-center the sliding joint using hydraulic means
DS R2	Large rocking residual drifts	Replace the column

Table 4. Repair times for conventional columns used in baseline system, as a function of damage state

DS	PB1 (days)	PB2 (days)	Dispersion
DS 1	0	0	0.00
DS 2	3	2	0.40
DS 3	9*	8*	0.56
DS 4	9*	8*	0.56
DS 5	13*	10*	0.47
DS 6	22*	18*	0.47

* Permitting needed.

Table 5. Repair times for other conventional bridge elements (used in both baseline and competing systems), as a function of damage

	Bearings		Backwall		Shear keys		Deck		All
DS	**PB1 (days)**	**PB2 (days)**	**PB1 (days)**	**PB2 (days)**	**PB1 (days)**	**PB2 (days)**	**PB1 (days)**	**PB2 (days)**	**Dispersion**
DS1	1*	1*	2	2	1	1	2	2	0.40
DS2	N/A[+]		3	3	2	2	2	2	0.40
DS3			7*	8*	14*	14*	N/A[+]		0.56
DS4			19*	22*	14*	14*			0.47

* If any of these DS occurs, add 3 days of time to account for temporary support. Permitting needed.
[+] Bearings only have one damage state; desk/superstructure only has two.

Table 6. Repair times for HSR columns

DS[+]	PB1 (days)	PB2 (days)	Dispersion
DS 1	3	2	0.40
DS 2	9	8	0.56
DS 3	14*	11*	0.47
DS 4 or DS R2	12*	8*	0.47
DS R1	1	1	0.40

[+] Segment DS and Residual drift DS times are added, except when the column is replaced (DS4/DS R2)
* Permitting needed.

Figures

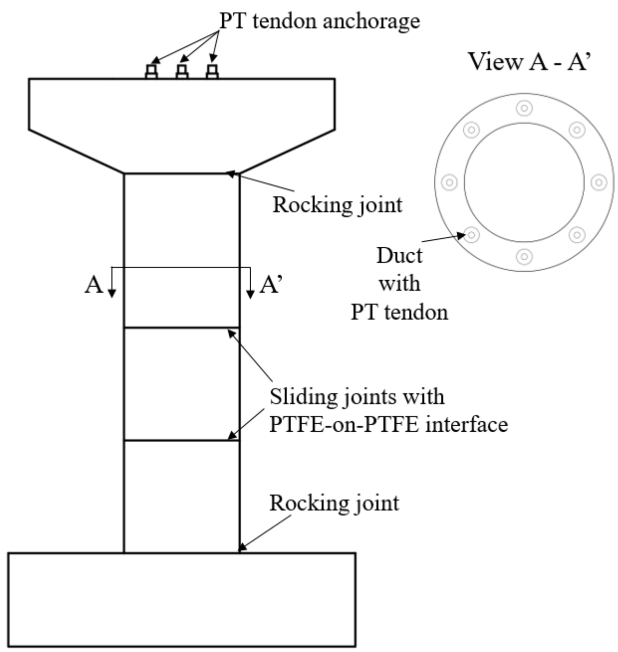

Figure 1. Schematic of Generation 2 HSR column, as tested by Valigura et al. (2019b) and Salehi (2019).

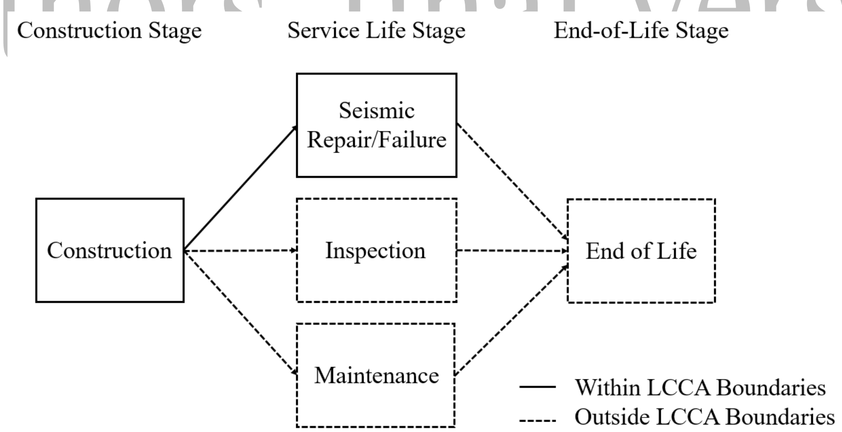

Figure 2. Bridge life-cycle stages, showing those considered within the boundaries of this assessment.

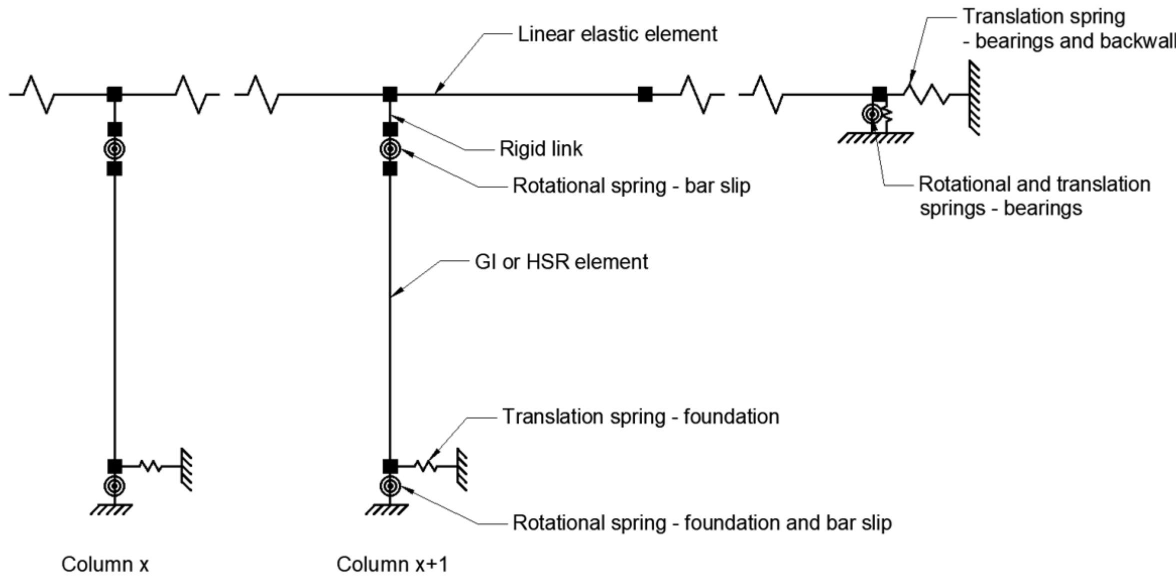

Figure 3. Schematic of analytical bridge model.

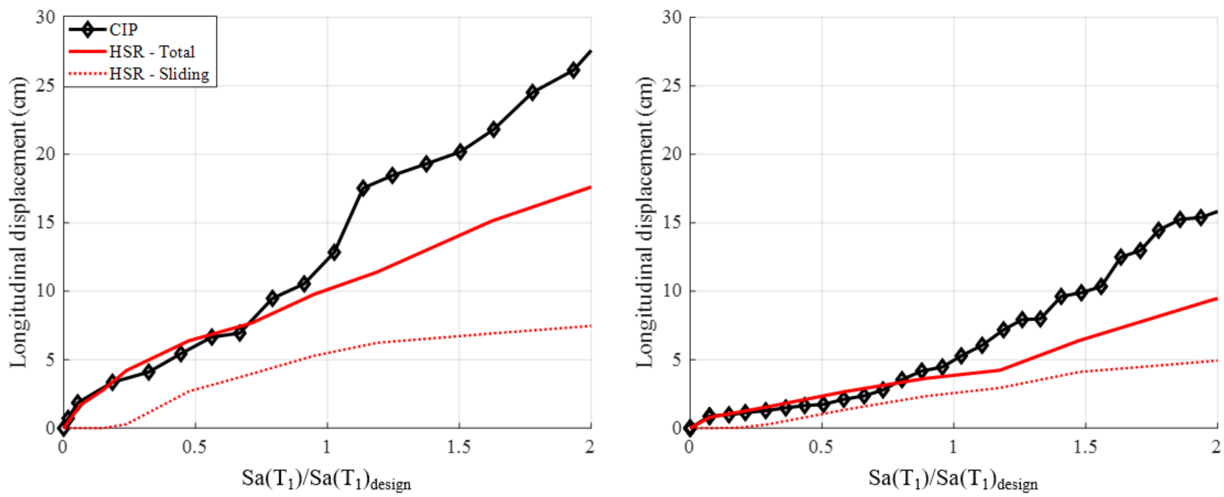

a) b)

Figure 4. Comparison of peak longitudinal displacements for baseline and competing bridge systems for: a) PB1 and b) PB2.

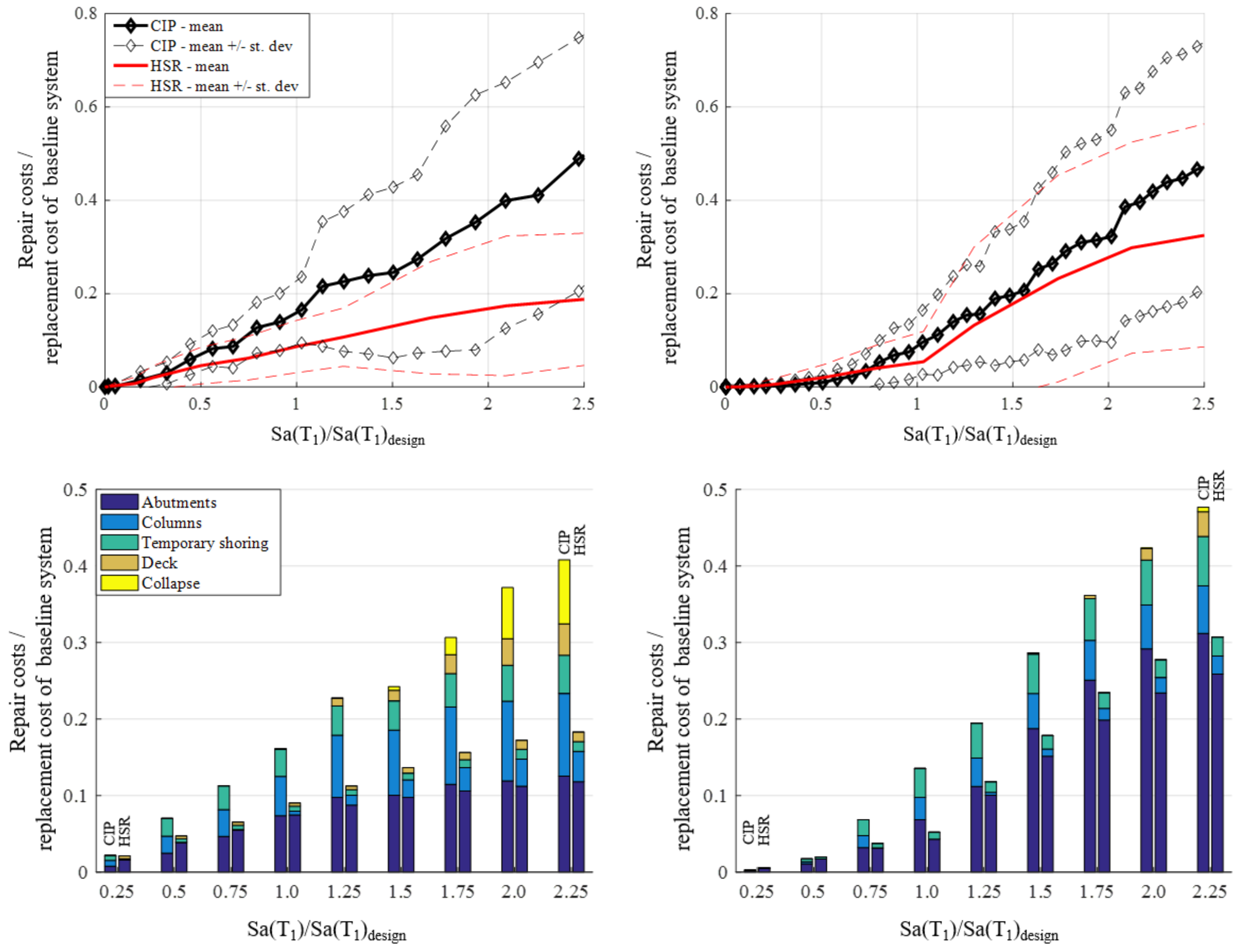

a) b)

Figure 5. Repair cost vulnerability curves and their deaggregation for baseline and competing bridge systems for: a) PB1 and b) PB2.

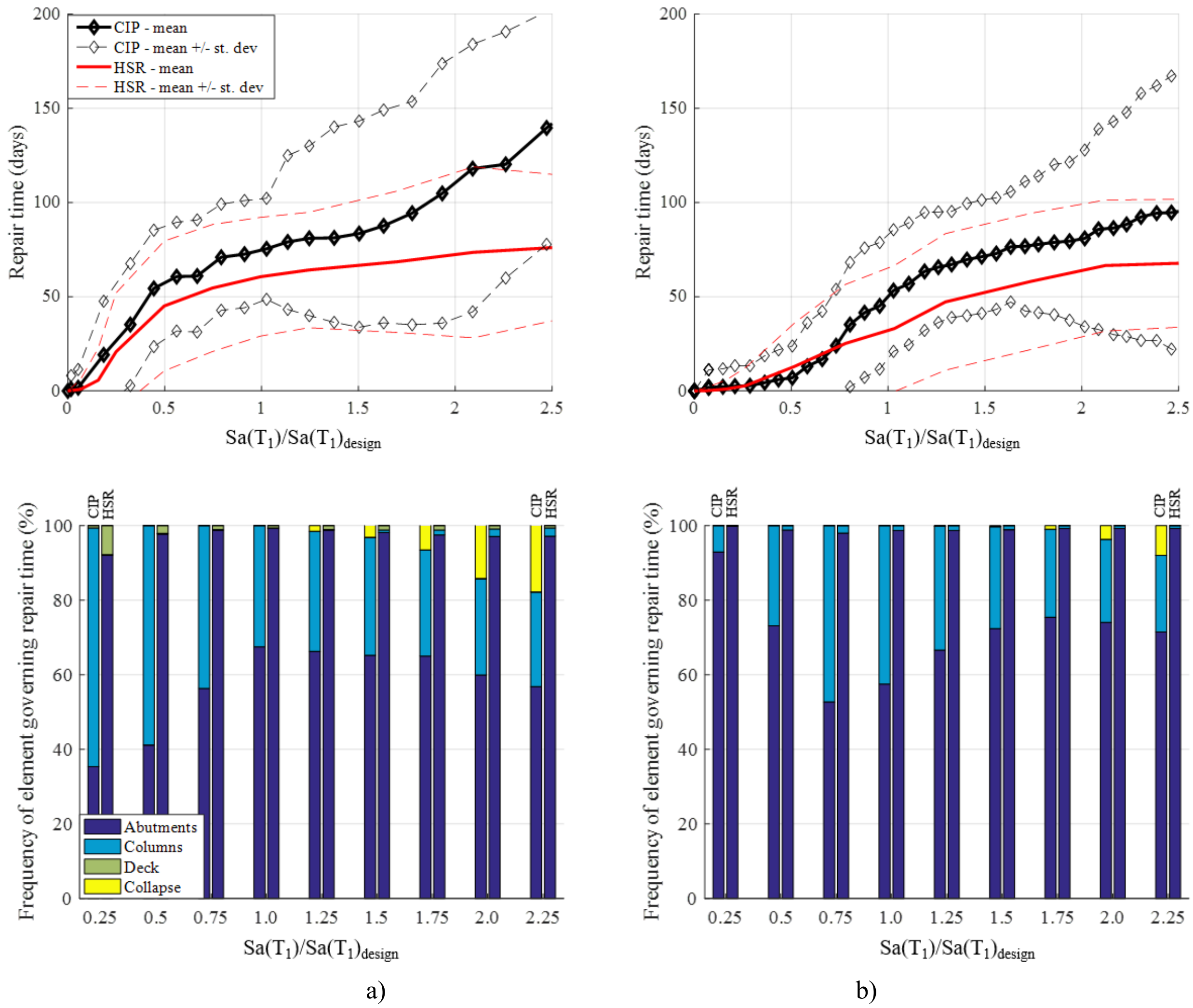

Figure 6. Repair time vulnerability curves and their deaggregation for baseline and competing bridge systems for: a) PB1 and b) PB2. The deaggregations show the percentage of realizations at given IM level for which the repair of a given type of element controls the repair time.

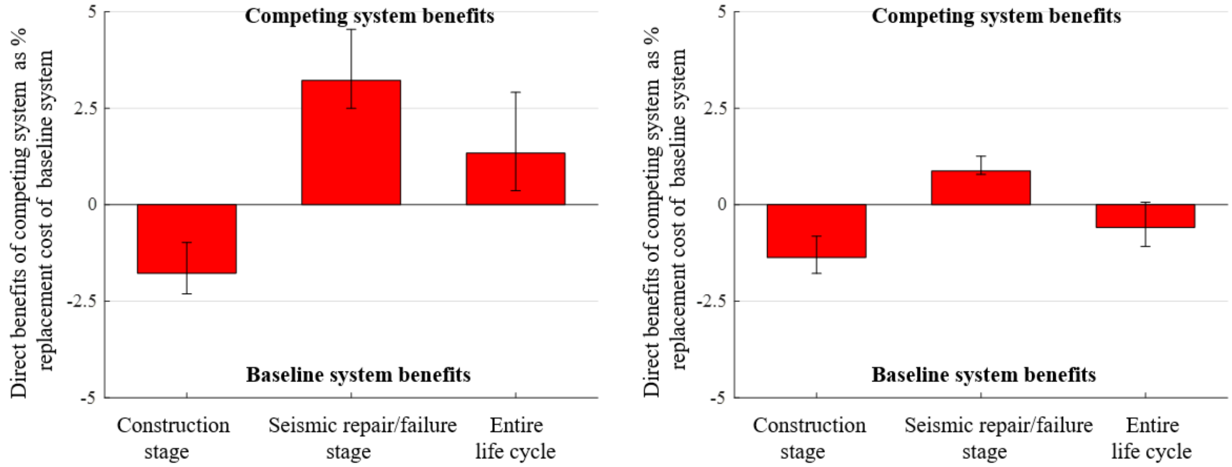

a) b)

Figure 7. Median benefits of competing system in terms of direct costs over construction, seismic repair/failure stages, and entire life cycle for: a) PB1 and b) PB2. The “error bars” show the 16th and 84th percentile results from uncertainty propagation.

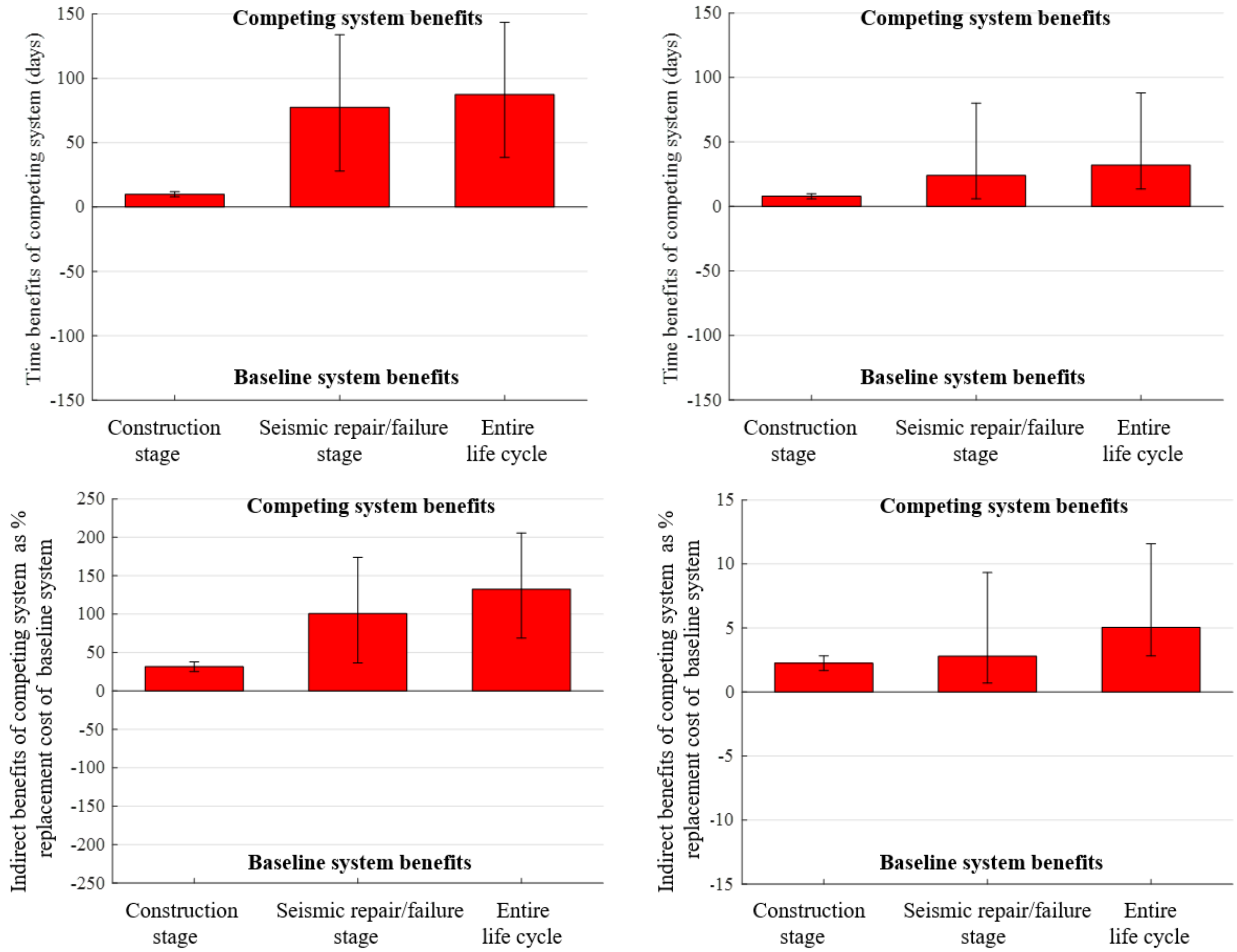

a) b)

Figure 8. Median benefits of competing system in terms of time (top) and corresponding indirect costs (bottom) over construction, seismic repair/failure stages, and entire life cycle for: a) PB1, and b) PB2. The "error bars" show the 16th and 84th percentile results from uncertainty propagation. Please note different scale of y-axis for a) and b) in the lower panel.

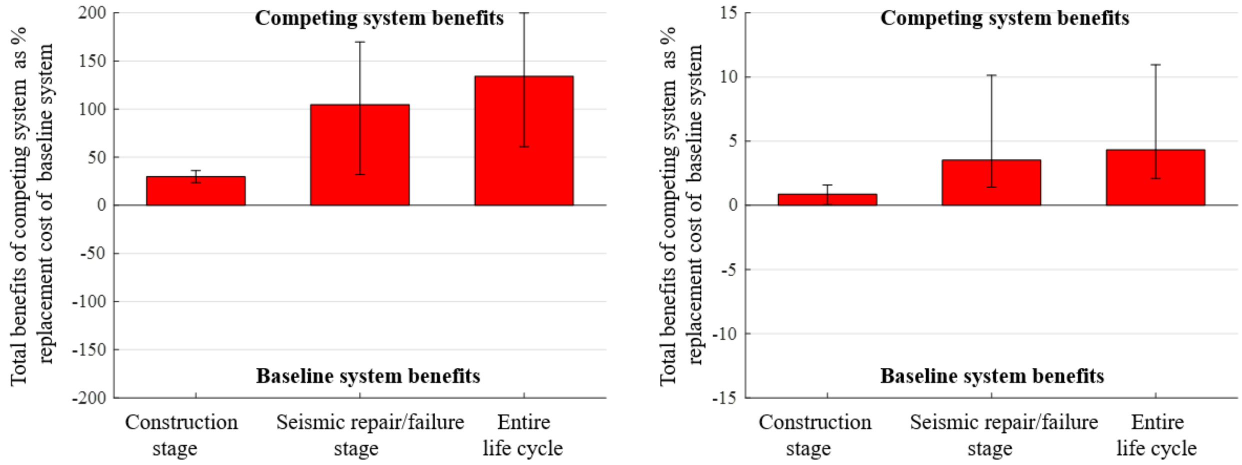

a) b)

Figure 9. Median benefits of competing system in terms of total direct and indirect costs for: a) PB1, and b) PB2. The "error bars" show the 16th and 84th percentile results from uncertainty propagation. Note different scale of y-axis for a) and b).

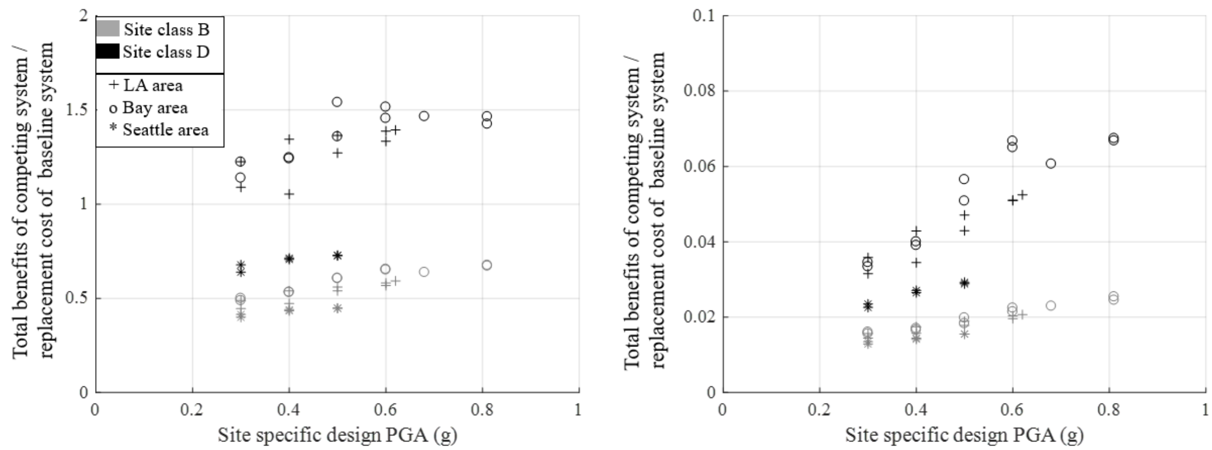

a) b)

Figure 10. Median benefits of competing system in terms of direct and indirect costs for 26 sites and site classes B & D for: a) PB1 and b) PB2. Site design PGA is a proxy for site seismic hazard/seismicity. Please note different scale of y-axis in a) and b).

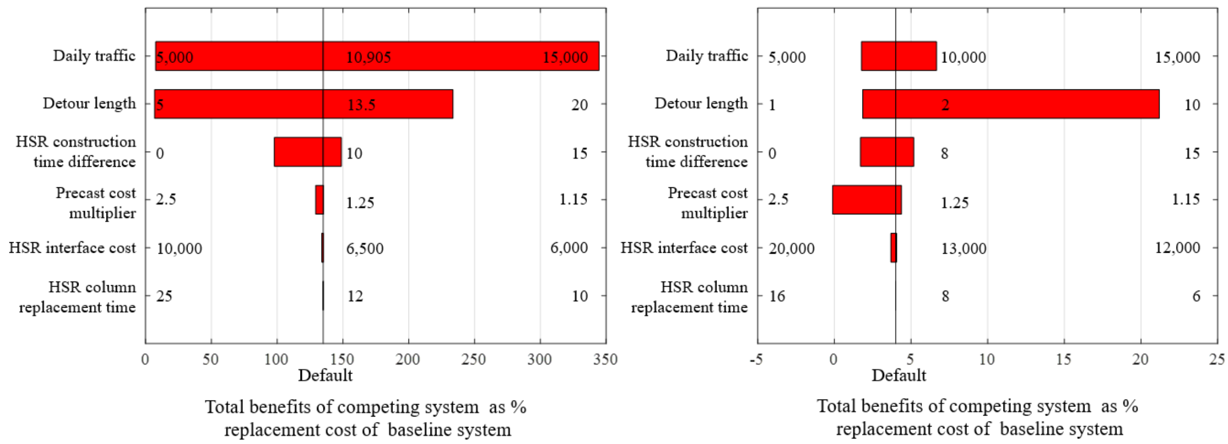

a) b)

Figure 11. Results of sensitivity study total benefits for: a) PB1 and b) PB2. Values on the left correspond to values least favorable to HSR columns, values on the right to most favorable to HSR columns, values in the middle are default values used throughout the study.

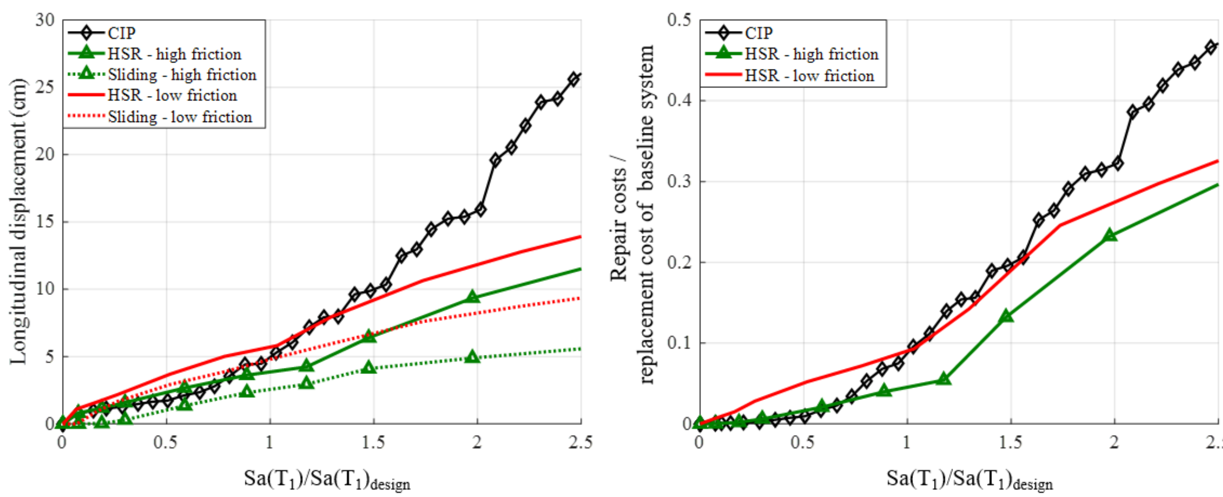

a) b)

Figure 112. Comparison among two different competing bridge systems with different onset of sliding and the baseline bridge system for PB2 in terms of: a) longitudinal peak displacement, and b) seismic repair costs. “HSR – high friction” are the results presented elsewhere in this paper for PB2-H.